Perception, control and path planning of robotic laparoscopic surgical system

Alexios Karadimos

Supervisor: Associate Professor, **Evangelos Dermatas**
Co-Supervisor: Professor, **Anthony Tzes**

Deparment of Electrical and Computer Engineering

Patras, February 2022

Outline

Surgical Robotics Procedure

Figure: DaVinci Xi, ©2020 Intuitive Surgical, Inc.

1. patient preparation
2. small incisions at the anatomical region of interest
3. trocars mounting
4. robot positioning, mounting & calibration of surgical tools
5. remote operation from special console

Advantages of Surgical robotics

for the patient, **Minimally Invasive**:

- Smaller incisions
- Less blood loss
- Reduced risk of inpatient infection
- Less pain
- Faster patient recovery

for the surgeon:

- Increased **precision** and reduced human errors: Smooth and precise movements, Detection and correction of errors caused by hand tremble
- **No fulcrum effect**
- Haptic feedback
- Teleoperation & ergonomics

Thesis goals

Study all the stages involved in the perception, control and manipulation of robotic laparoscopic tools with emphasis given to the **pivot trajectories and the RCM constrained motion planning**

- laparoscopic tool detection, calculation of relative position and orientation of the center of mass
- calculate the contact points on the tool
- calculate the path from the tools' table to the surgical table
- calculate the pivot trajectories that needs to be executed when the tool is inserted in the trocar

Outline

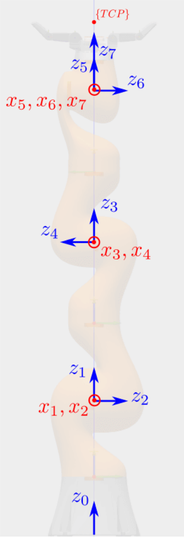

i	θ_i (rad)	L_{i-1} (m)	d_i (m)	α_{i-1} (rad)
1	θ_1	0	0.36	0
2	θ_2	0	0	$-\pi/2$
3	θ_3	0	0.36	$\pi/2$
4	θ_4	0	0	$\pi/2$
5	θ_5	0	0.4	$-\pi/2$
6	θ_6	0	0	$-\pi/2$
7	θ_7	0	0	$\pi/2$

Table: D-H parameters for Kuka iiwa14

$$^{i-1}T_i = \begin{bmatrix} c\theta_i & -s\theta_i & 0 & L_{i-1} \\ s\theta_i c a_{i-1} & c\theta_i c a_{i-1} & -s a_{i-1} & -s a_{i-1} d_i \\ s\theta_i s a_{i-1} & c\theta_i s a_{i-1} & c a_{i-1} & c a_{i-1} d_i \\ 0 & 0 & 0 & 1 \end{bmatrix}$$

Solve separately for position and orientation (assume $\theta_3 = 0$)

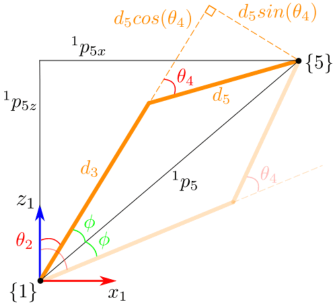

$$R_{target} = \begin{bmatrix} i_x & j_x & k_x \\ i_y & j_y & k_y \\ i_z & j_z & k_z \end{bmatrix}$$

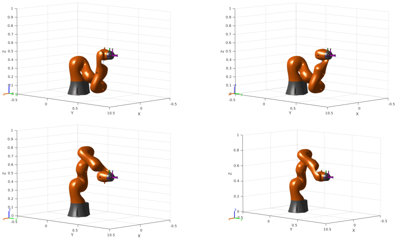

$${}^0\mathbf{p}_5 = {}^0T_4 {}^4\mathbf{p}_5 = \begin{bmatrix} p_x \\ p_y \\ p_z \end{bmatrix}$$

Figure: The first 4 out of 8 solutions of the IK-problem

Singularity points

- points where robot has **reduced kinematic capability**
  - cannot move in some directions
  - cannot move at all
  - points where small displacements/velocities in the taskspace require very large displacements/velocities in the joint space
  - kinematics equations are not defined or $\|J\| = 0$
- must be known before path planning in order **to be avoided**
- example singularity points (based on KUKA's Sunrise.OS 1.11 manual)
  - shoulder fully extended $\Rightarrow \theta_1$ and θ_3 are not defined (there are infinite combinations for the same result)
  - When $\sin(\theta_6) = 0$ then the angles θ_5, θ_7 are not defined. (infinite number of combinations of θ_5, θ_7 to get the same orientation on the end-effector.

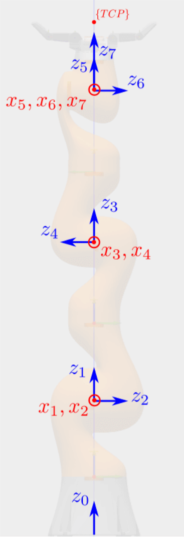

RCM constraint

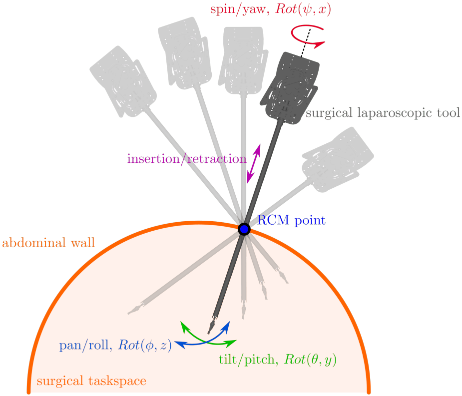

Figure: Illustration of pivoting motion of surgical laparoscopic tool around RCM point (also known as fulcrum or trocar point). Due to the RCM constraint, the tool has only 4 degrees of freedom.

Elbow-up constraint

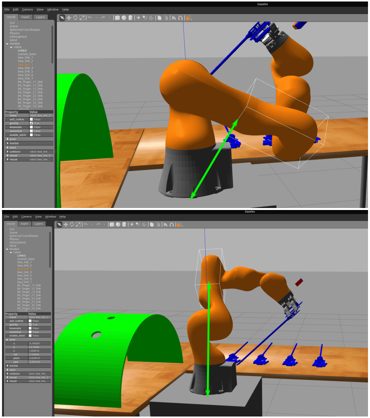

Figure: Top: elbow-down solution, bottom: elbow-up solution

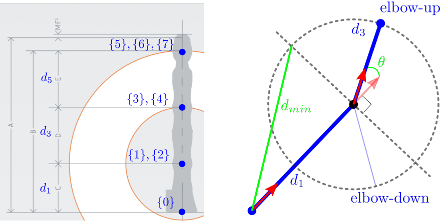

Figure: Elbow-up constraint description with relative distance or angle between links with lengths d_1 and d_3

$$d_{\min} \leq d \leq d_{\max}, \text{ where}$$
$$d_{\min} = \sqrt{d_1^2 + d_3^2} = 553\text{mm and}$$
$$d_{\max} = d_1 + d_3 = 780\text{mm}.$$

Outline

Gripper & Forward Kinematics

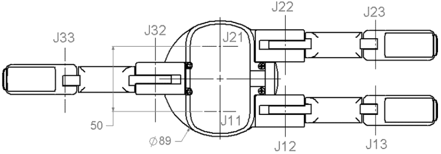

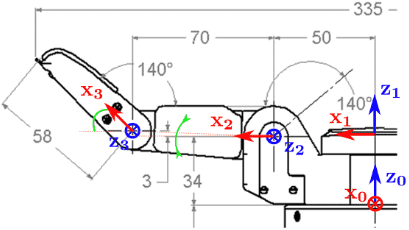

i	θ_i (rad)	L_{i-1} (m)	d_i (m)	α_{i-1} (rad)
1 (J11)	$\theta_{11} - \pi/2$	0.025	0.0034	0
2 (J12)	$\theta_{12} + 0.04$	0.05	0	$\pi/2$
3 (J13)	$\theta_{13} + 0.69$	0.07	0	0

i	θ_i (rad)	L_{i-1} (m)	d_i (m)	α_{i-1} (rad)
1 (J21)	$\theta_{21} - \pi/2$	0.025	0.0034	0
2 (J22)	$\theta_{22} + 0.04$	0.05	0	$\pi/2$
3 (J23)	$\theta_{23} + 0.69$	0.07	0	0

i	θ_i (rad)	L_{i-1} (m)	d_i (m)	α_{i-1} (rad)
1	$\pi/2$	0	0.0034	0
2 (J32)	$\theta_{32} + 0.04$	0.05	0	$\pi/2$
3 (J33)	$\theta_{33} + 0.69$	0.07	0	0

D-H parameters for **Barrett Hand BH8-282**

Gripper Inverse Kinematics

Standard solutions of a RRR kinematic chain, using the law of cosines

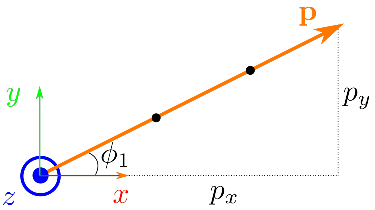

Figure: top view

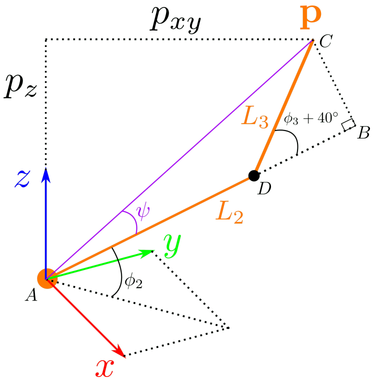

Figure: side view

Outline

Tool detection & pose estimation

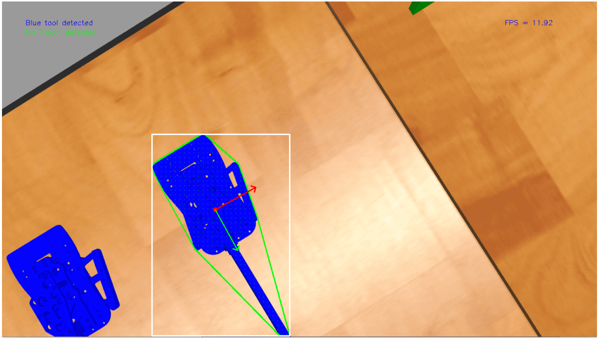

Figure: Tool's ROI, convex hull, center of mass and orientation vectors

$\mathbf{a}, \mathbf{b}$: orientation vectors, solutions of

$$\mathbf{C}\mathbf{v} = \lambda \mathbf{v}$$

$$\mathbf{C} = \begin{bmatrix} \sigma(x,x) & \sigma(x,y) \\ \sigma(y,x) & \sigma(y,y) \end{bmatrix}$$

$$(\bar{x}, \bar{y}) = \left(\frac{1}{N} \sum_{i=1}^{N} x_i, \frac{1}{N} \sum_{i=1}^{N} y_i \right)$$

$$\sigma(x,y) = \frac{1}{n-1} \sum_{i=1}^{N} (x_i - \bar{x})(y_i - \bar{y})$$

Calculation of grasping points

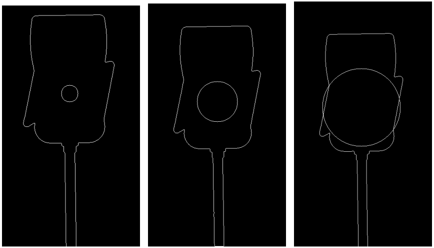

Figure: Finding candidate grasping points from the intersections of a growing circle mask $I_1(x, y)$ and the contour of the detected surgical tool $I_2(x, y)$

1. $\mathbb{G} = \underset{(x,y)}{\arg\max} I_1(x, y) \odot I_2(x, y)$
2. match points with stereo 3d points
3. check feasibility with gripper kinematics & force closure
4. repeat (grow circle) until all conditions are met

Outline

Tool pose

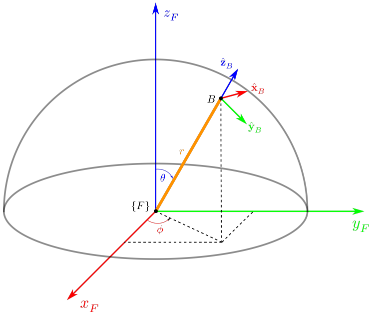

$$
{}^{F}T_B = \begin{bmatrix} {}^{F}R_B & {}^{F}\mathbf{p}_B \\ \mathbf{0} & 1 \end{bmatrix}
$$

where

$$
{}^{F}R_B = \begin{bmatrix} \hat{\mathbf{x}}_B & \hat{\mathbf{y}}_B & \hat{\mathbf{z}}_B \end{bmatrix}
$$

Calculate orientation vectors using spherical coordinate unit vectors

$$
\hat{\mathbf{x}}_B = \hat{\phi} = \begin{bmatrix} -\sin(\varphi) \\ \cos(\varphi) \\ 0 \end{bmatrix}
$$

$$
\hat{\mathbf{y}}_B = \hat{\theta} = \begin{bmatrix} \cos(\theta)\cos(\varphi) \\ \cos(\theta)\sin(\varphi) \\ -\sin(\theta) \end{bmatrix}
$$

$$
\hat{\mathbf{z}}_B = \hat{\mathbf{r}} = \begin{bmatrix} \sin(\theta)\cos(\varphi) \\ \sin(\theta)\sin(\varphi) \\ \cos(\theta) \end{bmatrix}
$$

The Fulcrum Effect

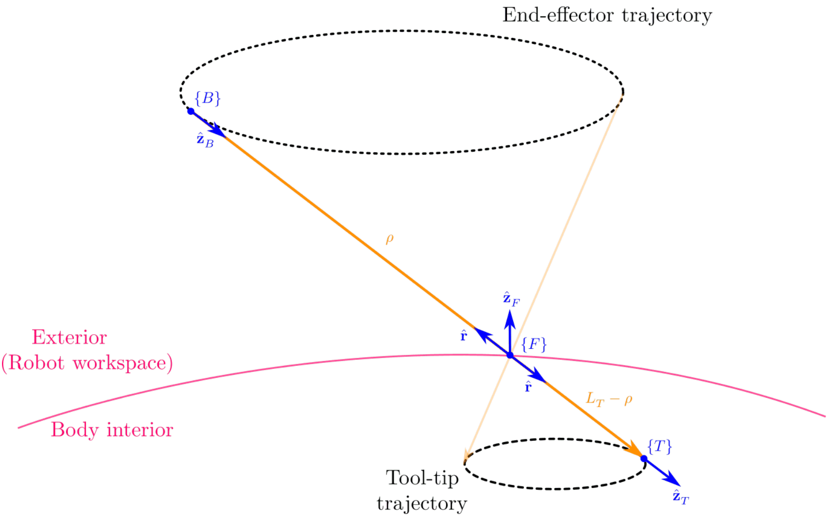

Line segment trajectory of tool tip

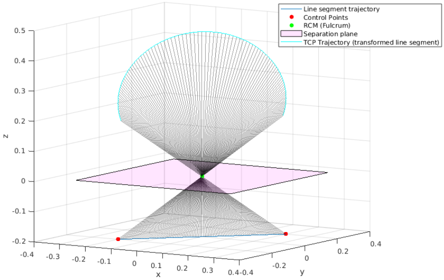

Figure: A Line segment trajectory and it's transformation due to the Fulcrum Effect

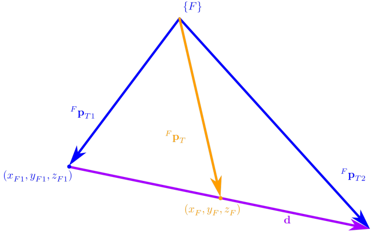

$$\begin{cases} x_F = (1-s)x_{F1} + sx_{F2} \\ y_F = (1-s)y_{F1} + sy_{F2} \\ z_F = (1-s)z_{F1} + sz_{F2} \end{cases}$$

Circular trajectory of tool tip

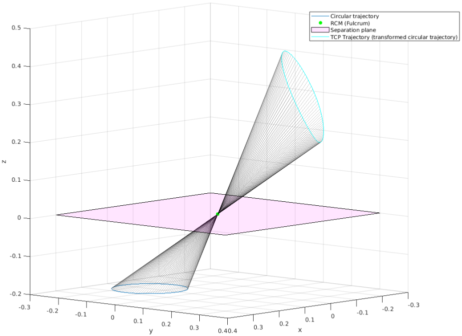

Figure: Circular trajectory of tool tip with respect to Fulcrum reference frame and it's transformation via the Fulcrum Effect

$$\begin{cases} x_F = r_0 \cos(2\pi s) + x_{F0} \\ y_F = r_0 \sin(2\pi s) + y_{F0} \\ z_F = z_{F0} \end{cases},$$

$$s \in [0, 1]$$

$$\begin{cases} r = \sqrt{x_F^2 + y_F^2 + z_F^2} \\ \theta = atan2\left(\sqrt{x_F^2 + y_F^2}, z_F\right) \\ \varphi = atan2(y_F, x_F) \end{cases}$$

Circular trajectory of tool tip

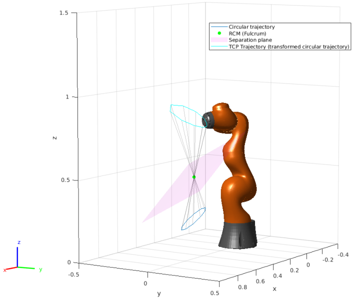

Figure: Circular trajectory that lies on an a plane of arbitrary orientation with respect to the fulcrum point

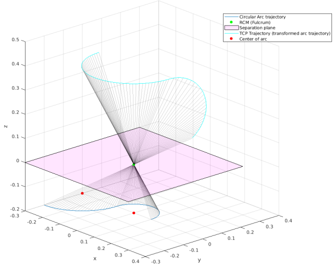

Figure: Circular arc trajectory of tool tip with respect to Fulcrum reference frame and it's transformation via the Fulcrum Effect. In this trajectory 2 circular arcs are used

Helical trajectory of tool tip

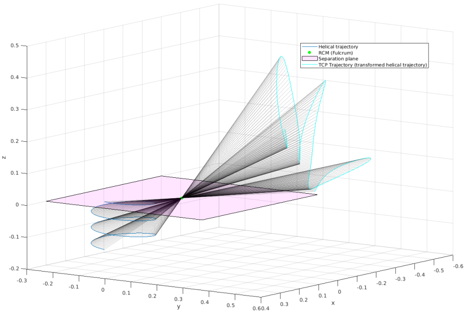

Figure: Helical trajectory of tool tip with respect to Fulcrum reference frame and it's transformation via the Fulcrum Effect

$$\begin{cases} x_F = r_0 \cos(2\pi s) + x_{F0} \\ y_F = r_0 \sin(2\pi s) + y_{F0} \\ z_F = \pm \beta s \end{cases}$$

$$s \in [0, \tau]$$

τ: cycles

β / r_0: slope (aka pitch)

Cubic Spline trajectory of tool tip

$$x_i(s) = a_i(s - s_i)^3 + b_i(s - s_i)^2 + \\ + c_i(s - s_i) + d_i$$

$$s_i \leqslant s \leqslant s_{i+1}$$

boundary conditions $\Rightarrow \alpha_i, b_i, c_i, d_i \in \mathbb{R}$

$$x_i(s_i) = x_i$$

$$x_i(s_{i+1}) = x_{i+1}$$

$$\dot{x}_i(s_i) = \dot{x}_i$$

$$\dot{x}_i(s_{i+1}) = \dot{x}_{i+1}$$

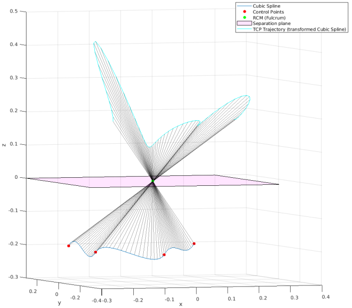

Figure: A Cubic Spline trajectory and it's transformation via the Fulcrum Effect

B-Spline trajectory of tool tip

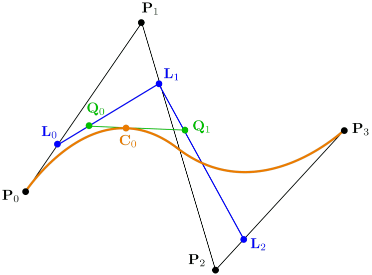

Figure: Cubic Bézier curve calculated using cubic interpolation of 4 control points

$$\mathbf{L}_0(s) = (1-s)\mathbf{P}_0 + s\mathbf{P}_1$$
$$\mathbf{Q}_0(s) = (1-s)\mathbf{L}_0(s) + s\mathbf{L}_1(s)$$
$$\mathbf{C}_0(s) = (1-s)\mathbf{Q}_0(s) + s\mathbf{Q}_1(s)$$

$$\mathbf{C}_0(s) = (1-s)^3\mathbf{P}_0 + 3(1-s)^2 s\mathbf{P}_1 + \\ + 3(1-s)s^2\mathbf{P}_2 + s^3\mathbf{P}_3$$

B-Spline trajectory of tool tip

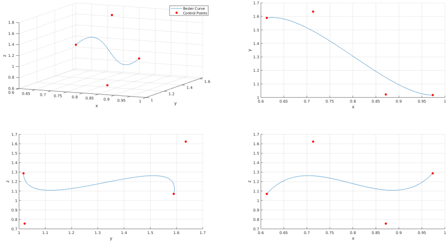

Figure: A cubic Bézier curve calculated and plotted in MATLAB

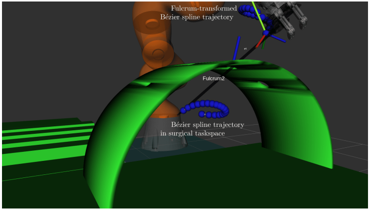

Figure: Experiment 3d: Create the B-spline trajectory inside the surgical site (below the green mounting dock) and transform it via the fulcrum transformation to a trajectory for the robot's TCP.

Trajectory planning in joints' space

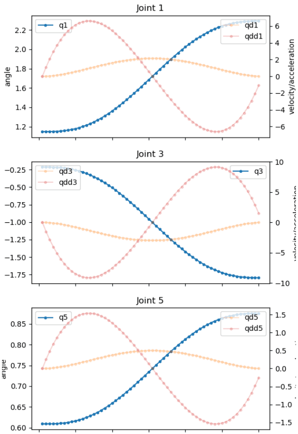

Figure: Quintic polynomial trajectories

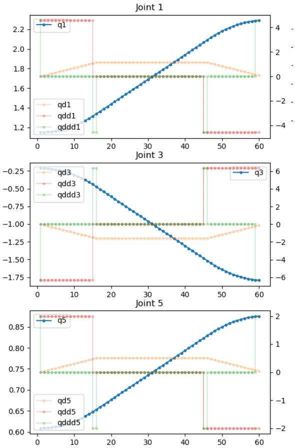

Figure: Trajectories with trapezoid velocity profile

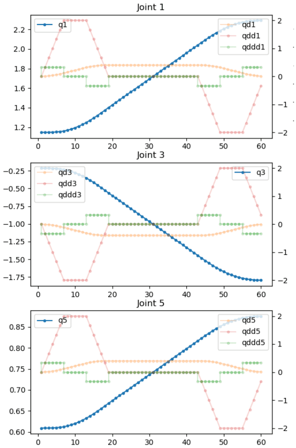

Figure: Trajectories with s-curve velocity profile

Outline

RCM Tracking

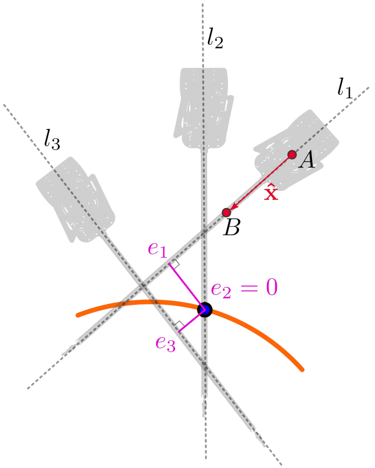

Figure: Geometric calculation of the RCM alignment error e using the distance between the line l and the RCM point.

$$^{U}T_{T0} = \begin{bmatrix} \hat{\mathbf{x}} & \hat{\mathbf{y}} & \hat{\mathbf{z}} & \mathbf{p} \\ 0 & 0 & 0 & 1 \end{bmatrix}$$

$$\overrightarrow{O_F A} = \mathbf{p}, \quad \text{and} \quad \overrightarrow{O_F B} = \mathbf{p} + \hat{\mathbf{x}}$$

$$e_{rcm} = d(l, O_F)$$

$$d(l, O_F) = \frac{\|\overrightarrow{O_F A} \times \hat{\mathbf{x}}\|}{\|\hat{\mathbf{x}}\|}$$

RCM Tracking

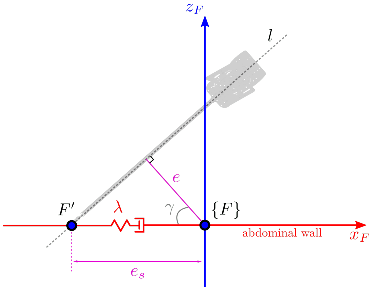

Figure: Force interaction model of the laparoscopic tool and the abdominal wall around the fulcrum point (RCM point)

$$\|\mathbf{f}_s\| = \frac{\lambda}{cos\gamma} e$$

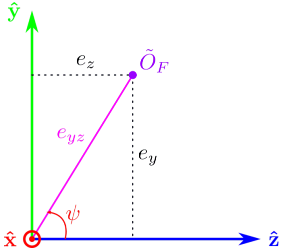

Figure: RCM error calculation in yz plane. The RCM error or yz-error is the distance between the line of the $\hat{\mathbf{x}}$ vector (here seen as a point) and the estimated position of the origin of the fulcrum reference frame $\tilde{O}_F$

RCM Tracking

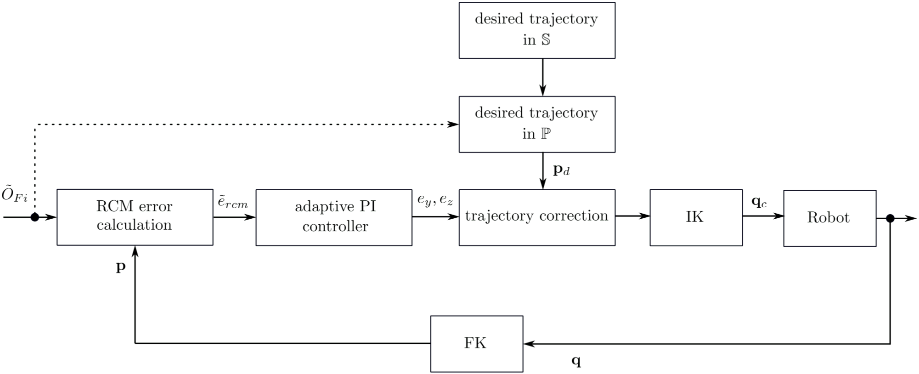

Figure: RCM tracking proposed control system. The RCM error is used as input in the trajectory generator to correct the trajectory command in order to fix the RCM misalignment

Image based visual servoing

Figure: Image based visual servoing. The robot arm is controlled using the information gained from the video frames. The frames are 2-Dimensional and thus the detected objects can have only 3 degrees of freedom which means we can mainly control 3 independent variables, here the x, y, θ variables. The left image is the initial frame and the right image is the frame where the object is at the target pose.

$$\mathbf{e}[k] = [e_x, e_y, e_\theta]^\top$$

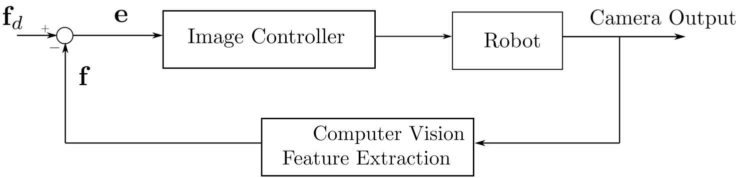

Figure: Image based visual servoing closed loop control

$$\mathbf{x}[k+1] = \mathbf{x}[k] + \mathbf{u}[k]$$

$$\mathbf{u}[k] = K_p \mathbf{e}[k] + K_i \sum_{i=0}^{k-1} \mathbf{e}[i] + K_d \left(\mathbf{e}[k] - \mathbf{e}[k-1] \right)$$

Firm grasping algorithm & Force control

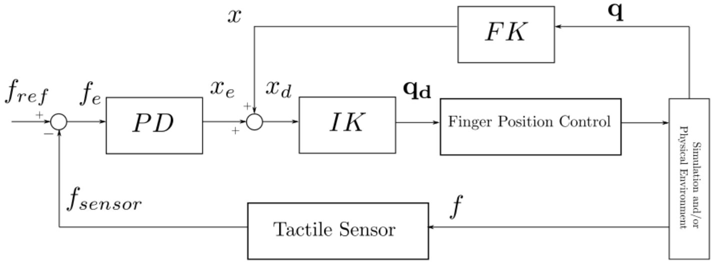

Figure: Force control on a Barrett Hand gripper finger

Outline

ROS framework

Key components:

- Nodes
- Topics & Messages
- Parameters
- Launch files
- Packages
- ROS filesystem, network, tools & community
- ...

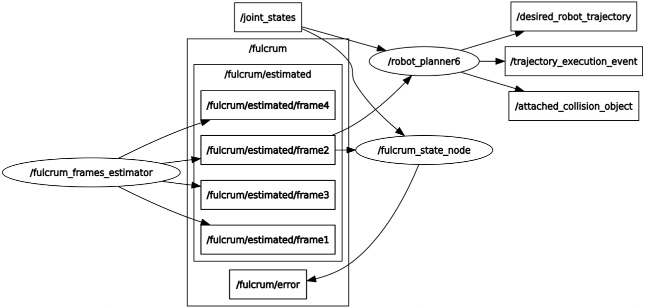

Figure: Subset of ROS nodes and topics used for the robot-planner6 experiment

Gazebo & RViz

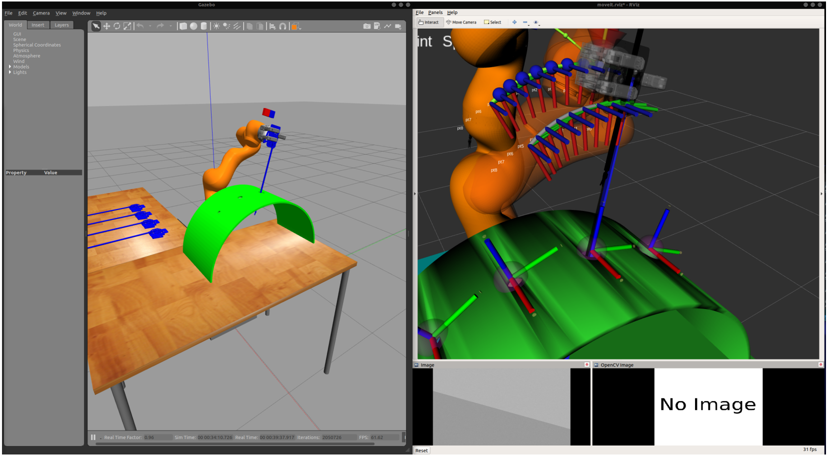

Figure: Simulation with Gazebo (physics engine, sensors, graphics etc.) & visualization with RViz (visualize robot state, known data such as topics or sensor measurements, markers, geometric objects etc.)

Motion Planning with Moveit

Moveit motion planning parameter values outside and inside of surgical site:

- **Position tolerance**: 50 - 500µm, 5µm
- **Orientation tolerance**: 0.00005deg, 0.000005deg
- **Maximum planning time**: 5-10s, 5s
- **Replanning allowed**: true
- End-effector **interpolation step**: 1mm
- **Base frame**: world (universal)
- **Jump threshold**
- **Planner algorithm**: RRTConnect
- **Maximum planning attempts**: 6
- **Fraction**

Tools, Packages and Libraries

- **tf2**: keep track of multiple coordinate frames, apply transformations
- **geometry_msgs**
- **Eigen**: linear algebra
- **OpenCV2**: computer vision
- **numpy**
- **actionlib**
- State machines with **Smach**
- ros-industrial/**kuka_experimental**
- **barrett_hand**
- **gazebo-pkgs**
- **moveit-pkgs**
- ...

Outline

Robot Planner 1: Simple MoveIt planning

Goal: Benchmark MoveIt Path planning algorithms

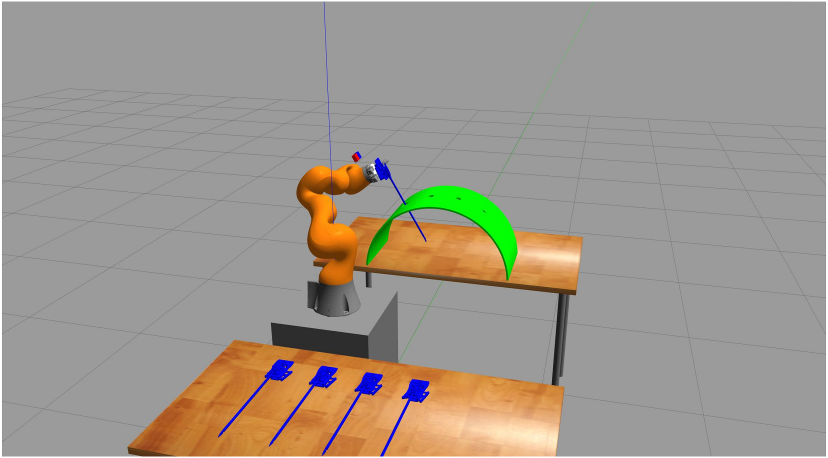

Robot Planner 1: Simple MoveIt planning

	RRTConnect			
	Insertion & Pivot trajectories			
10 Experiments	Insertion planning time	Execution status	Pivot planning time	Execution status
Average	0.163102	1	0.5014398	0.9
Standard deviation	0.110001	-	1.110582	-

	RRT*			
	Insertion & Pivot trajectories			
10 Experiments	Insertion planning time	Execution status	Pivot planning time	Execution status
Average	5.083449	0.9	5.090813	0.6
Standard deviation	0.066253	-	0.041338	-

Robot Planner 2: Simulation layout and reachability experiments

Goal: Find layout with better reachability

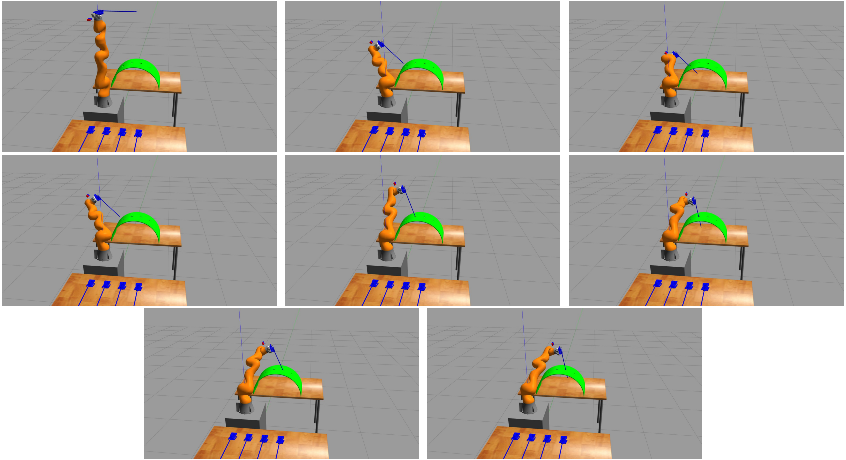

Figure: Experiment 2a: first layout

Robot Planner 2: Simulation layout and reachability experiments

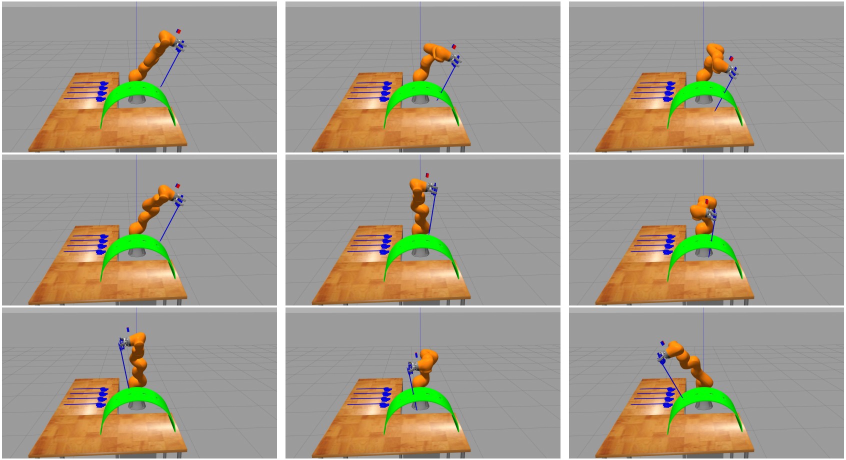

Figure: Experiment 2b: second layout

Robot Planner 2: Simulation layout and reachability experiments

Robot Planner 2a	RRTConnect			
	Insertion & Pivot trajectories			
10 Experiments	Trocar3 insertion time	Execution status	Trocar3 retraction time	Execution status
Average	0.298179	0.92	0.727752	0.237
Standard deviation	0.088385	-	0.314852	-

Robot Planner 2b	RRTConnect			
	Insertion & Pivot trajectories			
10 Experiments	Trocar3 insertion time	Execution status	Trocar3 retraction time	Execution status
Average	0.241715	1	1.364774	0.8
Standard deviation	0.107534	-	2.202951	-

Robot Planner 3b: Line segment trajectories in task space

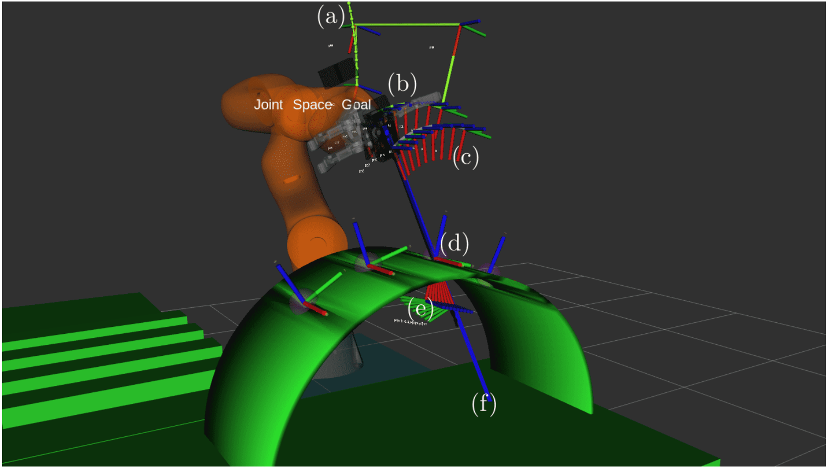

Figure: Experiment 3b

Robot Planner 3b: Line segment trajectories in task space

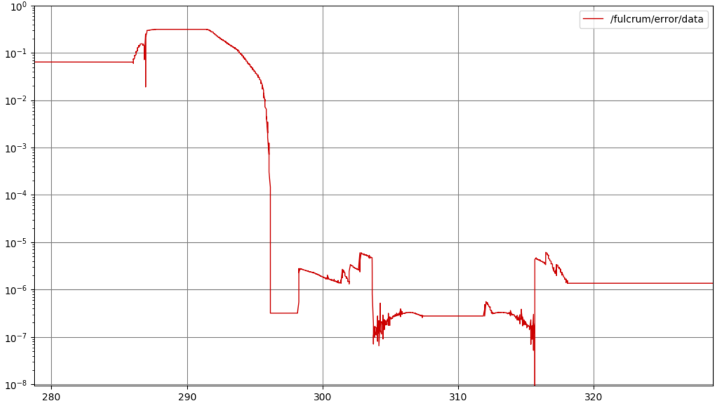

Figure: RCM error diagram from home position to line and reverse-line segment trajectories.

Robot Planner 3b: Line segment trajectories in task space

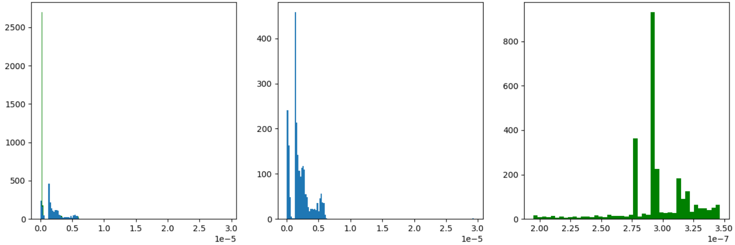

Figure: RCM error distributions, measurements from 10 iterations of the same experiment. From left to right: distribution of all measurements, distribution of measurements while the robot was pivoting, distribution of measurements while the robot was inserted but still.

	Average [m] (accuracy)	Standard Deviation [m] (repeatability)	sample size
while pivoting	$2.112649 \cdot 10^{-6}$	$1.609277 \cdot 10^{-6}$	2309
while inserted and still	$2.948652 \cdot 10^{-7}$	$2.948652 \cdot 10^{-7}$	2696

Line segment trajectories in task space

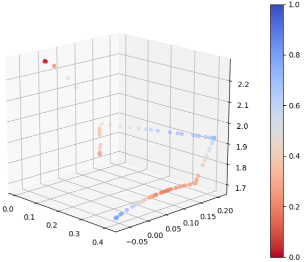

Figure: Experiment 3b: Manipulability plots of the whole trajectory the robot executed during 2 iterations of the same experiment

$$\mathcal{M} = \sqrt{det(JJ^{\top})}$$

Robot Planner 3b: Line segment trajectories in task space

Robot Planner 3b	Approach and **line segment pivot** trajectories with **RRTConnect**			
	elbow-up preparatory path			
10 Experiments	Elbow-up Start pose planning time (sec)	Execution status	Elbow-up preparation path planning time (sec)	Execution status
Average	0.174222	1	0.117040	1
Standard deviation	0.049002	-	0.084238	-
	Approach & Insertion			
10 Experiments	Approach fulcrum 2 path planning time (sec)	Execution status	Insertion path planning time (sec)	Execution status
Average	0.116498	1	0.249556	1
Standard deviation	0.088078	-	0.078941	-
	Line segment pivot trajectories			
10 Experiments	Line segment path planning time (sec)	Execution status	Reverse line segment path planning time (sec)	Execution status
Average	1.809001	1	5.356607	0.7
Standard deviation	2.421448	-	0.086818	-

Robot Planner 3a: Circular and Circular arc trajectories in task space

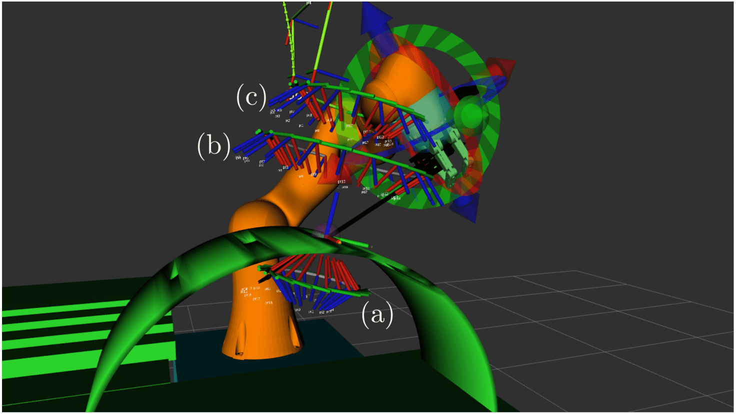

Figure: (a) The original circular trajectory designed inside the surgical taskspace, (b) the transformed trajectory that the base of the surgical tool will follow, (c) the actual transformed trajectory that the robot's end-effector will follow

Robot Planner 5: Visual servoing

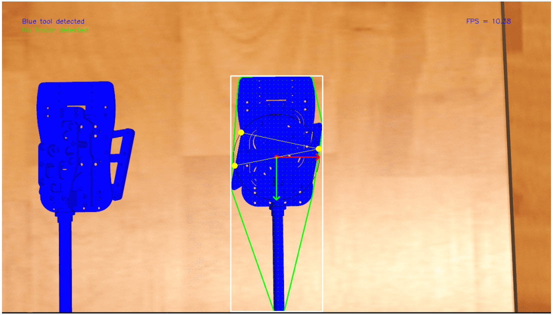

Figure: Image based visual servoing and calculation of grasp points. The yellow points are the grasp points and the thin black circumscribed circle is the growing circle that was used to calculate them.

Robot Planner 5: Visual servoing

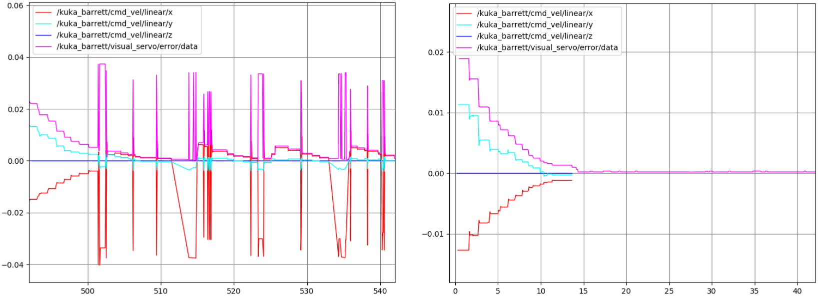

Figure: Visual servo controller error diagrams. On the left image in the error graphs appear some spikes. These spikes occur from the sudden temporary detection of a nearby surgical tool. On the right image, these spikes are filtered out, and only the error graphs of the visual servoing of one tool are shown. The controller parameters are $K_p = 0.9, K_d = 0.2$

Robot Planner 7: State machine - End-to-end simulation

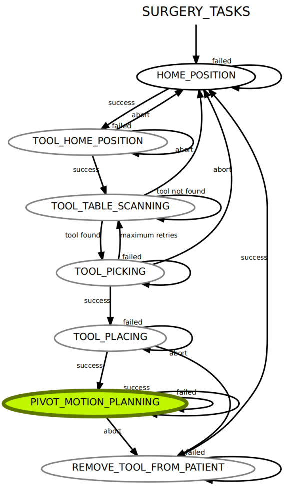

Run all the stages of this thesis together (integration testing) using a state machine.

Demo

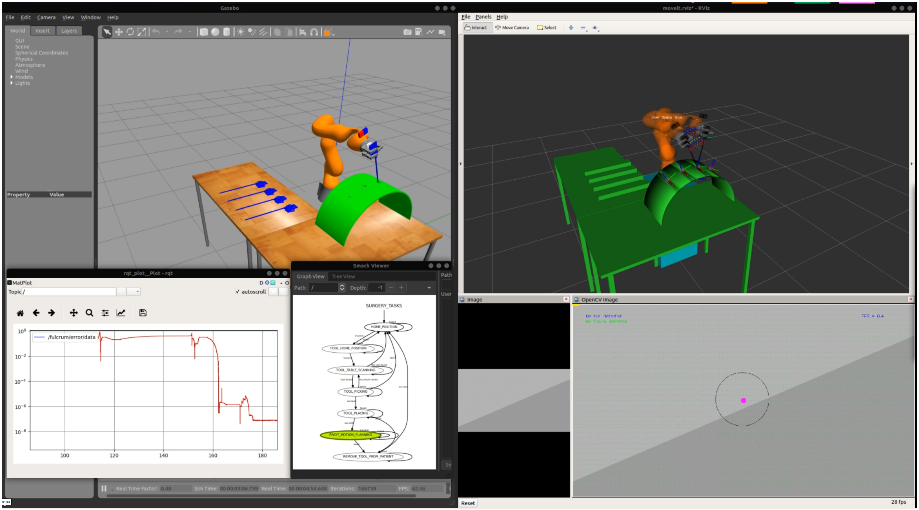

https://youtu.be/lfV1vdHf7bk

Outline

Conclusions

Surgical robotics critical requirements:

- Positional accuracy
- Orientation accuracy
- Time optimization
- RCM constraint
- Interpolation accuracy
- Collision avoidance
- Suitable path planning algorithms
- Repeatability
- Good environment layout and robot base position
- Good reachability of trajectories
- Singularity avoidance
- Jump threshold
- Fulcrum position and orientation
- Firm surgical tool grasping

Future Work

- Simulation and interaction with deformable bodies
- Advanced visualization and Haptics feedback
- Using the trajectories from chapter 6 as building blocks for more complicated trajectories like suturing
- Multiple robot arm collaboration: designing pivot trajectories for 2 or more robot arms
- Advanced grasping of gripper and/or laparoscopic tool's tip

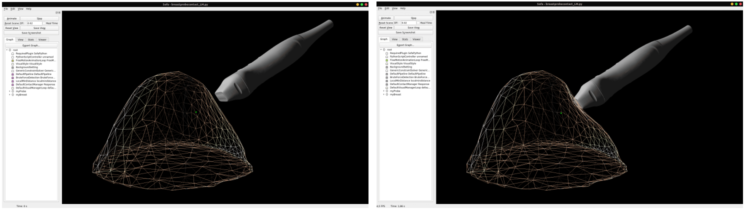

Figure: Soft tissue interaction, deformable objects simulation with the SOFA Framework

Code & Documentation

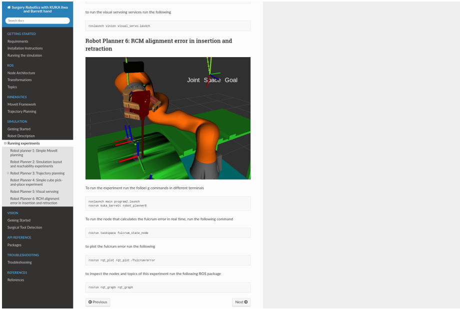

- Git repository: **https://github.com/karadalex/surgery_robotics_kuka_barrett**
- Documentation: **https://karadalex.github.io/surgery_robotics_kuka_barrett/**

Questions?

Thank you,

up1046820@upnet.gr
karadalex@gmail.com